

Epoxy + liquid crystalline epoxy coreacted networks: II. Mechanical properties

Prakaipetch Panchaipetch^a, Veronica Ambrogi^{a,b}, Marta Giamberini^b, Witold Brostow^a,
Cosimo Carfagna^b, Nandika Anne D'Souza^{a,*}

^aDepartment of Materials Science, University of North Texas, Denton, TX 76203-5310, USA

^bDepartment of Materials and Production Engineering, University of Naples Federico II, Piazzale Tecchio 80, 80125 Naples, Italy

Received 22 May 2001; received in revised form 29 August 2001; accepted 31 August 2001

Abstract

The effect of coreacting diglycidyl ether of bisphenol F (DGEBP-F) with diglycidyl ether of 4,4'-dihydroxybiphenol (DGE-DHBP) on mechanical properties is investigated. DGE-DHBP shows a liquid crystal (LC) transition upon curing. Tensile, impact and fracture toughness test results are evaluated. Dynamic mechanical analysis is conducted to determine the effect of the DGE-DHBP component. Scanning electron microscopy of fracture surfaces shows changes in failure mechanisms compared to the pure components. The results indicate that the mechanical properties of these blended samples are significantly improved at 10–20% by weight of DGE-DHBP. This is a consequence of the rigidity of the LC component which thus provides the reinforcement. © 2001 Elsevier Science Ltd. All rights reserved.

Keywords: Epoxy; Polymer liquid crystals; Fracture toughness

1. Introduction

Epoxy resins are an important component of advanced polymer matrix composites. There have been many efforts to improve the mechanical properties of epoxy resins [1–9]. A multiphase toughening mechanism is an effective way to produce high toughness epoxies. Introduction of functionalized reactive rubbers and thermoplastics are two common approaches. Typically, 5–20% reactive rubber by weight is incorporated into an epoxy matrix. This idea has been applied to reactive rubbers like carboxyl, amine or epoxy terminated butadiene acrylonitrile (CTBN, ATBN, or ETBN) [10–13]. The other elastomeric modifiers studied include acrylates [14,15], poly(oxypropylene amines) [16,17], and polysiloxane copolymers [2]. The fracture toughness of modified epoxy resins is typically higher than that of unmodified ones. However, the blends show adverse effects in decreased upper use temperatures, lower stiffness and strength [2,18,19]. Furthermore, the rubber toughening approach of thermosets fails in high temperature applications. Toughening of such blends involves a chemically induced phase separation process. One starts from a single homogeneous phase of rubber and host matrix. A low

molecular weight liquid rubber, which can dissolve in the epoxy resin, is usually first blended and dispersed into the epoxy matrix. However, the components separate out during the curing process. The degree of chemical interaction between the resin and rubber particles, as well as the rubber particle sizes, affect the interfacial adhesion and toughness [4].

Modification of epoxies with thermoplastics provides an alternative approach, which avoids the problems seen in toughening epoxies by rubber. Important properties such as modulus, yield stress, and glass transition are not adversely affected by the addition of a modifier. However, toughening epoxies with thermoplastics presents significant problems in processing due to large viscosity differences between the thermoplastic and epoxy. Epoxy resins blends, with non-modified thermoplastics such as poly(ether sulfone) and poly(ether imide), have been studied by Bucknall [20] and Diamont [21]. No significant improvement was reported. In contrast, thermoplastics with reactive terminal groups have been found to improve the fracture toughness while having little effect on other properties [22–25].

We infer from the above that the ideal epoxy matrix should have a high glass transition temperature and simultaneously a high toughness. Kinloch also supports the need to develop tough thermosets without sacrificing high glass transition temperatures for high performance applications

* Corresponding author. Tel.: +1-940-565-2979; fax: +1-940-565-4824.
E-mail address: ndsouza@jove.unt.edu (N.A. D'Souza).

[4]. Light weight, high performance and high T_g epoxy resins can serve in important applications as matrices for aerospace and integrated electronic circuit industries.

There is an interest in liquid crystal (LC) thermosets because of the combination of desirable properties from a thermoset and a LC [26]. LC epoxy resins (LCERs) are thermosets that have been investigated for at least a decade [27–29]. These materials combine the advantages of both LCs and epoxies, making them feasible matrices for advanced composites, and in electronic packaging [30,31]. As compared to ordinary epoxies, crosslinked LCERs have higher fracture toughness [29,32]. This can be explained by their approximately overall isotropic properties, combined with localized anisotropy. The inhomogenities of the LC structure leads to the deviation of crack propagation, thus, an increase in fracture toughness.

The potential for using LCERs for improving the mechanical properties of epoxy matrices was examined by Sue et al. [33]. They utilized reactive groups of 4,4'-dihydroxy- α -methylstibine (DHAMS) blended with diglycidyl ether of 4,4'-dihydroxy- α -methylstilbene (DGE-DHAMS) and cured with sulphanilamide as the matrix resins. Improved fracture toughness and modulus over a tough epoxy network resulted from the presence of liquid crystallinity. A blend of DGE-DHAMS with phenolic novolac resin cured with sulphanilamide also resulted in an improvement of mechanical properties.

In this paper we examine the potential of co-reacting DGEBP based epoxy and LCER of the same epoxy equivalence weight in the presence of an anhydride curing agent. In Part I, we have determined autocatalytic curing parameters of the network. The glass transition temperatures of the resulting networks using the differential scanning calorimeter was determined [34]. Here, we develop a plausible explanation for the creation of a single network by examining the solubility parameters of the individual components. High and low strain rate mechanical tests are coupled to examination of post failure fractography. The failure mechanism of cracks in the resulting coreacted network is investigated to help understand the toughening mechanism.

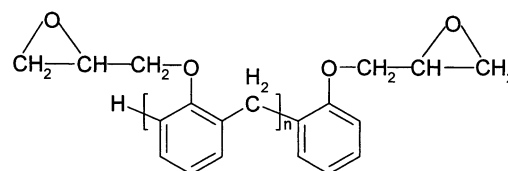
2. Experimental

2.1. Materials

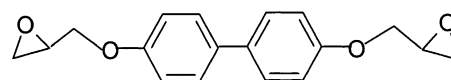
The epoxy resin used in this study is a low viscosity diglycidyl ether of bisphenol F (DGEBP-F) (Shell EPON862[®]) with an epoxy equivalence weight (EEW) in the range of 166–177. Pre-catalyzed methyltetrahydrophthalic (MTHPA) anhydride (Lindride-6[®]) is the curing agent. The anhydride equivalent weight is in the 165–175 range.

The LCER we have used is the diglycidyl ether of 4,4'-dihydroxybiphenol (DGE-DHBP). The synthesis procedure

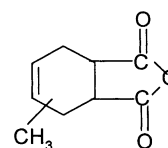
is described in Part I [34]. DGE-DHBP has the melting point of 153°C. The epoxide equivalent weight is 166. The mesogenic unit length is about 0.72 nm. The LC phase has not been found for the uncured sample. This interpretation is based on the results of Hefner and coworkers [35] who reported the absence of the LC phase earlier. The nematic LC phase was formed during curing. The chemical structures of all materials are shown as follows:



DGEBP-F



DGE-DHBP



MTHPA

2.2. Sample preparation

Pure components of DGEBP-F and blends of various concentrations of DGE-DHBP were prepared. The synthesized DGE-DHBP were dried and ground by mortar. Samples referred to as 'isotropic' reflect the absence of a liquid crystalline transition in the post cured state. The isotropic sample-curing schedule was as follows. Both epoxies were mixed in various concentrations and cured simultaneously with MTHPA at 1:1 stoichiometric ratios, at 120°C for 2 h, and then at 170°C for 1 h under vacuum. All the samples prepared for DMA, tensile, impact and fracture toughness tests were cured the same way. A nematic liquid crystalline sample was obtained by step curing the mixtures of DGE-DHBP and MTHPA. The mixtures were first melted at 80°C for 2 h and the curing temperatures were gradually increased to 100°C linearly for 1 h.

2.3. Dynamic mechanical analysis

Dynamic moduli and glass transition temperatures of the networks as a function of concentration of DGE-DHBP were investigated for compositions of 0, 10, 20, 30, 40, 50, 60, 80, and 100% of pure DGE-DHBP with DGEBP-F cured with MTHPA at 120°C for 2 h, and postcured at

170°C for 1 h under vacuum. DMA measurements were performed on a Perkin–Elmer DMA-7 apparatus using a three-point bending fixture. Measurements were run from 25 to 250°C at the heating rate of 10 K/min at 1 Hz frequency. Nitrogen was the carrier gas, with the flow rate of 20 ml/min.

Secondary transitions of unmodified and modified samples were investigated by a Rheometrics Dynamic Spectrometer RDS-IIe in the torsional mode. The constant strain amplitude was 1% with the constant frequency of 1.6 Hz. The experiments were performed from –150 to +210°C with the heating rate of 3°C/min.

2.4. Tensile tests

Pure components and blends were prepared for tensile measurements according to the ASTM D5937-96 standard with the type 1A dog-bone shape. The tests were performed using a MTS testing machine with the 2000 lb load cell and 1 mm/min. crosshead speed. Strains were determined with the aid of a gauge extensometer.

2.5. Impact tests

Impact measurements were measured with a Dynatup Impact Tester with 200 lb weight. Sample size 12 × 60 × 4 mm were prepared for Izod impact tests according to ASTM D5941-96. The 1.2 mm V-shaped sharp notch on each sample was precisely cut as an initiator point and then the natural crack generated by a fresh razor blade across the notch root. The impact strength was thus evaluated as a function of composition.

2.6. Fracture toughness

Fracture toughness was measured by the single notch procedure according to ASTM D5045-96. Sample specimen dimensions of thickness × length × width = 5 × 70 × 10 mm were prepared to ensure the state of plane strain at crack tips.

The samples with 0, 10, 20, 30, and 50% DGE-DHBP were prepared for single edge notch bending (SENB). The cured samples were cut with a 45° notch-cutting machine. The sharp notches were further cut with a diamond saw. The natural sharp crack was produced with a fresh razor blade. The sharp crack in all samples was prepared to ensure a valid result. The ratio of the crack length, a , to the sample width, W , of samples was in the range of 0.45–0.55 to ensure the condition of plane strain. The three point bending test was performed on an MTS testing machine with the displacement rate of 1 mm/min with a suspension span of 50 mm at room temperature. The load–displacement curves were used in calculations. The critical-stress-intensity factor, K_{IC} , and fracture energy, G_{IC} , values were obtained as functions of composition. K_{IC} is important to estimate the maximum load capacity while G_{IC} is a measure of the energy absorption.

The critical stress intensity in plane strain, K_{IC} , which represents the toughness of sample, is calculated as

$$K_{IC} = \frac{P}{B\sqrt{W}} f\left(\frac{a}{W}\right) \quad (1)$$

where P is peak load which represents the moment of crack extension, B is specimen thickness, and $f(a/W)$ is the correction factor, and a represents the specimen crack length. The geometric correction factor [36,37] is obtained from

$$f\left(\frac{a}{W}\right) = \frac{3 \frac{S}{W} \sqrt{\frac{a}{W}}}{2 \left(1 + 2 \frac{a}{W}\right) \left(1 - \frac{a}{W}\right)^{3/2}} \times \left[1.99 - \frac{a}{W} \left(1 - \frac{a}{W}\right) \left\{ 2.15 - 3.93 \left(\frac{a}{W}\right) + 2.7 \left(\frac{a}{W}\right)^2 \right\} \right] \quad (2)$$

The dimension of samples for valid K_{IC} values has to fulfill the condition

$$B, a, (W - a) > 2.5 \left(\frac{K_{IC}}{\sigma_y} \right)^2 \quad (3)$$

where σ_y is the yield stress of the material.

The critical strain energy G_{IC} was calculated as

$$G_{IC} = \frac{(1 - \nu^2) K_{IC}^2}{E} \quad (4)$$

where ν is the Poisson ratio and E is the tensile modulus of the sample.

2.7. Double edge notch four point bending

The samples for double-notch four point bending (DN-4PB) were prepared following the method used by Sue et al. [12,38,39]. DN-4PB was performed to observe the characteristic crack tip of unmodified and modified epoxy samples compared with the cured LCERS. The sample specimen dimensions were thickness × length × width = 5 × 70 × 10 mm. Samples were prepared by curing a stoichiometric ratio of the epoxy and the curing agent in a vacuum oven. Double notches were cut with a diamond saw, followed by a fresh razor blade.

The samples were tested by four-point bending using a MTS testing machine with cross-head speed of 0.5 mm/min until one section was broken. The section that did not break was used for the crack tip damage zone study. A small section from the middle was cut perpendicularly to the notch. The thin section was polished by 200 grit SiC paper, followed by 1 μm diamond paste with ethylene glycol. An optical microscope was used to observe the area around the crack tip.

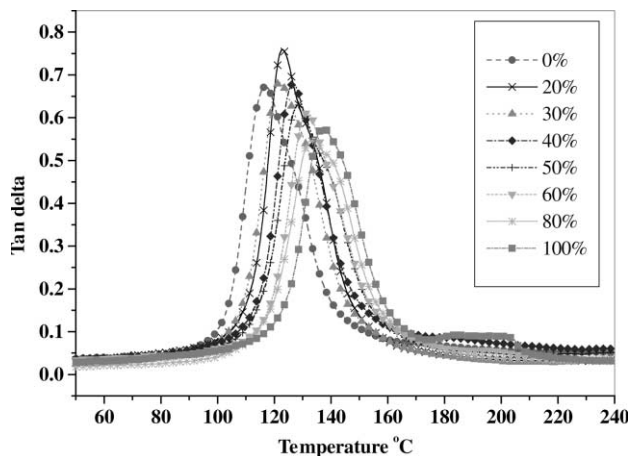


Fig. 1. Comparison of tan delta results as a function of DGE-DHBP concentration obtained from DMA.

2.8. Scanning electron microscopy

The morphologies of the fracture surfaces after tensile tests for each composition were observed using a JEOL T300 scanning electron microscope (SEM) at 15 kV accelerating voltage. Samples for each composition were cut to 2 mm heights. Each sample was mounted on a sample holder using an electrically conductive paint as an adhesive and coated with a thin gold layer by plasma sputtering to avoid a charging effect due to non-conductivity of the polymer.

3. Dynamic mechanical analysis

Tan δ curves as a function of temperature determined for several concentrations of the DGE-DHBP system are shown in Fig. 1. As the DGE-DHBP concentration increases, T_g

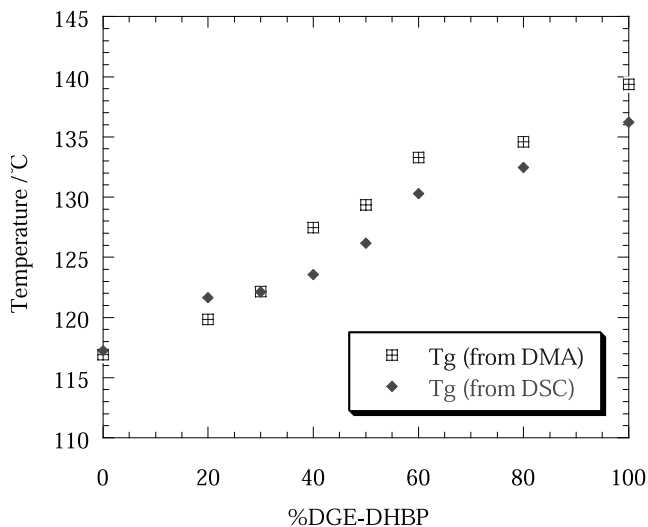


Fig. 2. Comparison of experimental and theoretical T_g values obtained from DSC and DMA.

also increases. T_g or α -transition of cured epoxy is the indication of rotational freedom in the segment between cross-links [40].

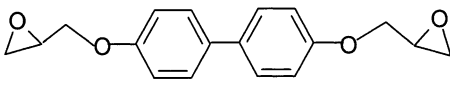
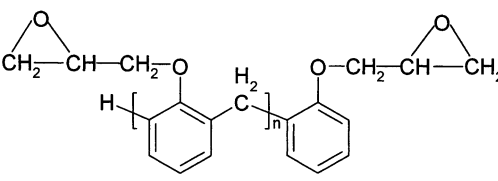
Results indicate a single network formed for the entire composition range of blended samples. Moreover, the areas under tan delta and loss modulus curves are higher for low DGE-DHBP concentrations. Fig. 2 presents the comparison of T_g obtained from DMA and DSC results as a function of DGE-DHBP concentration. The T_g values observed from DSC are lower than those from DMA but follow the same trend. As the DGE-DHBP concentration increases, a single intermediate T_g of the blended samples is observed. With reference to T_g 's of the pure system, the T_g of the network increases with DGE-DHBP concentration. This can be related to the similarity between the two constituent networks.

The solubility parameter was calculated based on the group contribution method recalculated by Coleman [41] as shown in Table 1. The solubility parameter calculation is based on the molar volume V^* and molar attraction constant P^* obtained by the least square methods. This was calculated based on the data base compiled by Daubert and Danner [42]. The calculated solubility parameter values are compared. The difference in solubility parameter values is $1.23 \text{ (J/cm}^3\text{)}^{0.5}$ from the pair of DGE-DHBP and DGE-BP-F. The similar structure of these epoxies leads to the similarity of the solubility parameters. Both epoxy resins have the same functionality, except that the functional groups are connected in different order.

The similarity in solubility parameter for the DGE-DHBP and DGE-BP-F leads to a high possibility of mutual dissolution of these two monomers. Moreover, the exothermic reaction during epoxy curing also enhances the possibility of a miscible system. The exothermic conditions of curing reactions ensure the miscibility of these blends and are based on the basic idea from the Flory–Huggins theory for exothermic reactions. Flory and Huggins predict that the condition of miscibility is always satisfied in such systems no matter how large the molecular weights. The miscibility observation will be confirmed from the detection of glass transition temperature of blends in Section 4.

Fig. 3 shows the dynamic mechanical spectra of loss moduli for 0, 10, 30, 50, and 100% DGE-DHBP from the RDS. Two distinct peaks are observed at -80 and 110°C , representing the β -transition and glass transition temperatures, respectively. The β -transitions can be assigned to side chain or pendant group movements. In epoxy systems, the β -relaxation transition is associated with $-\text{CH}_2\text{CH}(\text{OH})-\text{CH}_2\text{O}-$ segments of the cured molecule [43,44]. The strength of the β -transition is related to the efficiency of epoxy in absorbing energy, as reflected in mechanical and acoustic properties [45,46]. As DGE-DHBP concentration increases, the secondary molecular motion is more pronounced. The T_g of the blend tends to increase as DGE-DHBP concentration in the system increases. The T_g value obtained from DSC, DMA and RDS show the same

Table 1
The solubility parameter calculation by group contributions method

Structure	Functional group	V^* (cm ³ /mol)	F^* ((J cm ³) ^{0.5} /mol)	δ ((J/cm ³) ^{0.5})
 DGE-DHBP	–CH ₂ –	16.5	270	20.56
	>CH–	1.9	47	
	–O–	5.1	194	
	–C ₆ H ₅ –	75.5	1503	
 DGEBP-F	–CH ₂ –	16.5	270	20.29
	>CH–	1.9	47	
	–O–	5.1	194	
	–C ₆ H ₅ –	75.5	1503	

trend, namely T_g increases as a function of DGE-DHBP concentration.

The temperature used to cure LCER affects the LC phase stability as observed from time–temperature–transformation (TTT) diagram. The LC phase of cured product is stable only in a certain temperature range [47–49]. The effects of the curing conditions on dynamic mechanical properties are also compared. DGE-DHBP cured with MTHPA at 120°C produced an isotropic phase while the nematic phase is found in curing the sample at 90°C. The comparison shows that the isotropic sample has higher T_β . Its T_g is higher than for 0% DGE-DHBP but is lower than for other compositions.

The value of $\tan \delta$ from 20% DGE-DHBP modified sample is higher than for the unmodified sample. For DMA, the work input per unit volume or energy dissipation, W , is directly proportional to the loss modulus or $\tan \delta$ [50]

$$W = \pi \gamma_0^2 E'' \quad (5)$$

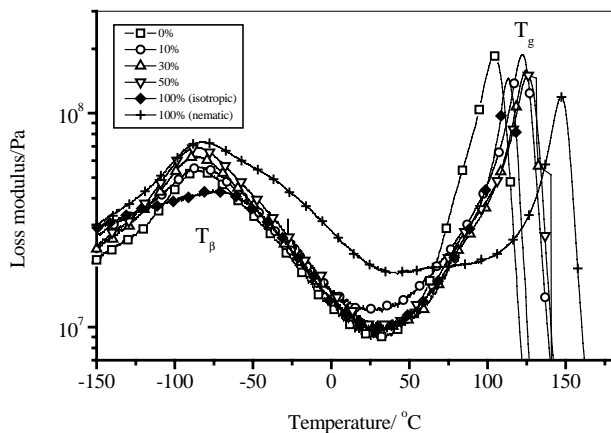


Fig. 3. Comparison of loss modulus values for several DGE-DHBP concentrations and curing temperature observed from RDS.

$$W = \pi \gamma_0^2 E' \tan \delta \quad (6)$$

where γ_0 is the strain amplitude, E' is the storage modulus and E'' is the loss modulus.

The DMA results indicate a higher energy dissipation from 20% DGE-DHBP compared with 0% DGE-DHBP sample. The dynamic modulus curves for cured epoxies consist of three main regions. The first is the glassy region, which has a modulus value in the range of several GPa. In the transition region, there is a sudden drop of modulus from 10^9 to 10^7 Pa. The modulus in the rubbery region (E'_R) is in the 10–20 MPa range. This plateau is related to the permanent bonding. The modulus value can quantify the crosslinking density. A relationship of E_R and crosslinking density has been derived in the classical rubber elasticity [51]. Tobolsky [52] has obtained the following relationship:

$$E'_R = \frac{3\varphi dRT}{M_x} \quad (7)$$

If the effect of dangling bonds is neglected, we have

$$M_x = \frac{d}{\rho} \quad (8)$$

where M_x is the molecular weight between crosslinks (g/mol), d is the polymer density (g/cm³) and ρ is the concentration of network chains (mole/cm³).

Thus, from Eqs. (4)–(9) we obtain

$$E'_R = 3\varphi\rho RT = 3\varphi k_B T \quad (9)$$

where E'_R is the modulus in the rubbery state, φ is the front factor which is close to unity, R is gas constant, k_B is Boltzmann constant, T is temperature in degrees K, and ρ is the crosslinking density.

Table 2 shows the comparison of E'_R as a function of the DGE-DHBP concentration. There is an increase in the E'_R on addition of the DGE-DHBP but the values do not change with composition within our range. The increase in modulus

Table 2

The comparison of T_{β} , T_g , loss modulus at room temperature and modulus at rubbery regions obtained from RDS

% DGE-DHBP	T_{β} (°C)	T_g (°C)	$E_{(T=200^{\circ}\text{C})}$ (Pa)
0	-84.6	104.8	10.6×10^6
10	-84.0	122.1	13.7×10^6
30	-87.1	124.5	13.9×10^6
50	-85.5	125.9	13.6×10^6
100 (isotropic)	-75.7	113.2	10.6×10^6
100 (nematic)	-84.1	146.8	14.9×10^6

in the rubbery region as a function of the DGE-DHBP concentration is due to the effect of rigid molecules. Mesogenic units enhance the crosslink density of the coreacted network; especially in the condition that allows orientation of mesogenic units before complete curing as seen in the nematic sample. For the DGE-DHBP sample, which was cured under isotropic conditions, imposed orientation was absent. Therefore, E'_R is of the same magnitude as for the pure DGEBP-F sample. Nematic samples however showed higher E'_R by 40% compared with those resulting in isotropic phases. For the network based on rigid units, modification based on enthalpic deformations need to be included in the rubber elasticity theory. The finite extensibility of LC units affects the entropic response to the applied force. In the isotropic sample, there is no preferred direction, by definition. Thus, the crosslinks can move in all directions when force is applied. For nematic samples, the molecules are restricted in the direction perpendicular to the director. Therefore, the network can only move in direction approximately parallel to the director.

4. Mechanical test results

Table 3 shows a summary of results from tensile, impact and fracture toughness tests as a function of DGE-DHBP concentration. The comparison of modulus, tensile strength, failure strain, and area under the stress–strain curve, indicates an improvement of toughness as 10 or 20% of DGE-DHBP is added. This result is also seen in microscopic mechanical DMA results (Fig. 1).

Selected stress vs. strain curves as a function of DGE-DHBP concentrations are presented in Fig. 4. The deformation comprises of a linear and a non-linear region. For the 10% DGE-DHBP sample a distinct yielding characteristic is found. As Table 3 shows the modulus of blends with two maxima, one around 10% and the other about 50% of DGE-DHBP, followed by a decreasing trend.

Thus, first we have the reinforcement of the DGEBP-F by the presence of the DGE-DHBP component. Then, we seem to exceed the θ limit, the concentration at which the LC component manifests its effect, a phenomenon analyzed before in terms of the generalized statistical mechanical model of Flory [53] and also seen experimentally in thermoplastic polymer liquid crystals (PLCs) [54,55]. When the

Table 3
Comparison of mechanical properties from tensile, impact and fracture toughness test for each % DGE-DHBP (v is assumed equal to 0.38; note: all the deviation results (\pm) of mechanical properties are obtained from the standard deviation calculation)

% DGE-DHBP	Tensile modulus (Gpa)	Tensile strength (Mpa)	Failure strain (%)	Toughness index	Impact strength (kJ/m ²)	Fracture toughness (Mpa/m ^{1/2})	Fracture energy (J/m ²)
0	2.51 ± 0.21	59.46 ± 6.57	3.42 ± 0.82	1.25 ± 0.50	0.83 ± 0.11	1.03 ± 0.09	294
10	2.88 ± 0.15	69.29 ± 0.74	4.93 ± 1.24	2.54 ± 0.92	1.18 ± 0.13	1.65 ± 0.16	556
20	2.62 ± 0.12	62.38 ± 6.04	3.35 ± 0.74	1.31 ± 0.52	1.00 ± 0.12	2.31 ± 0.15	802
30	2.89 ± 0.26	62.55 ± 8.59	3.14 ± 0.80	1.28 ± 0.56	1.05 ± 0.10	1.71 ± 0.04	681
50	3.18 ± 0.22	64.36 ± 3.35	2.61 ± 0.45	1.04 ± 0.16	0.77 ± 0.08	1.56 ± 0.20	441
80	2.57 ± 0.16	62.34 ± 3.93	3.35 ± 0.54	1.26 ± 0.32	0.94 ± 0.09	–	–
100	2.59 ± 0.19	49.68 ± 4.11	2.42 ± 0.22	0.68 ± 0.11	0.75 ± 0.11	–	–

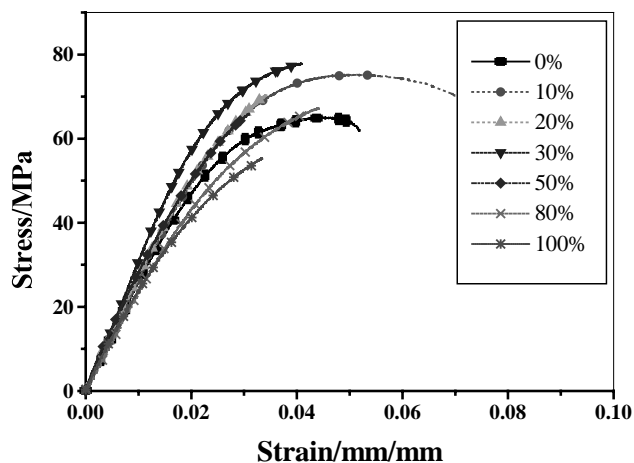


Fig. 4. Stress vs. strain curves for several concentrations of the DGE-DHBP in DGEBP-F system.

concentration of DGE-DHBP increases, the modulus initially increases and the compositions between 0 and 50% are enhanced by the effectiveness of the bridged network. Above 50% of the DGE-DHBP component, the material becomes gradually brittle and the modulus decreases, an effect we have also seen in thermoplastics PLCs [56]. The results show improvement of tensile strength and failure strain at low concentrations of DGE-DHBP. However, the area under the curve does not increase for samples containing more than 30% by weight DGE-DHBP.

The comparison of impact strength or energy required to break the sample as a function of the DGE-DHBP concentration is also tabulated in Table 3. The results correspond to the area under the curve obtained from tensile tests. The impact strength-composition results show two maxima for DGE-DHBP concentrations below 50% — and for the same reason. However, the second maximum occurs at a lower DGE-DHBP concentration than on the modulus diagram. This is a consequence of the higher sensitivity of impact testing to the brittleness introduced by the rigid units of the DGE-DHBP. Noting the error bars, we can see the differences are however small.

The critical stress intensity in plane strain, K_{IC} , which represent the toughness of the sample, is reported in Table 3. The K_{IC} values for blended samples increase as a function of the concentration of DGE-DHBP added, especially for 10 and 20% DGE-DHBP. However, the toughness decreases after 30% DGE-DHBP has been added. The improvement in fracture toughness is due to the inhomogeneities of anisotropic rigid biphenyl functional groups in DGE-DHBP molecules. We have found a two-fold increase in toughness when 20% DGE-DHBP is blended with DGEBP-F. The fracture toughness improvement from this system is lower compared with thermoplastic modified epoxy and reactive rubber modified epoxy systems. Martinez [57] found a three-fold increase in K_{IC} for polysulfone-modified diaminodiphenyl methane cured diglycidyl ether of bisphenol A (DGEBP-A). However, there is difficulty in processing this

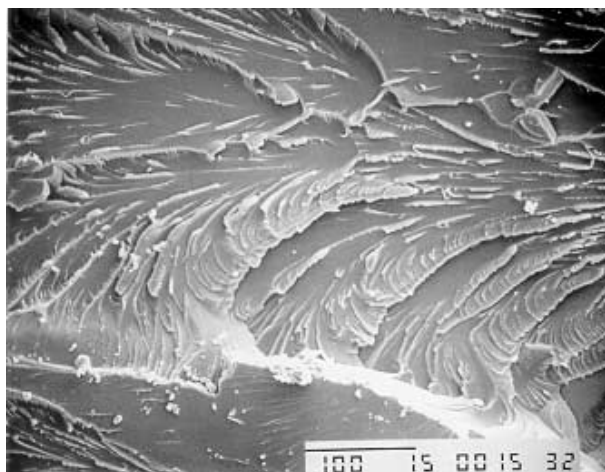


Fig. 5. Fracture surface of DGEBP-F (scale: 100 μm).

material because of different viscosities of thermoplastics and the epoxy. Pearson [58] has reported that the incorporation of carboxyl terminated random copolymer of butadiene and acrylonitrile increases fracture toughness of this epoxy by a factor of three. However, some desirable intrinsic properties, including strength and stiffness of the modified materials, are lowered by the inclusion of elastomeric materials.

Fracture energies increase when DGE-DHBP is added to the pure DGEBP-F — as seen in Table 3. The value of G_{IC} doubles when 20% DGE-DHBP is added.

5. Fractography

The fracture surfaces were investigated by SEM to support the mechanical results. Fig. 5 represents the fracture surface of DGEBP-F while the respective surface of DGE-DHBP is shown in Fig. 6. Typically three main regions are seen, namely initiation, propagation, and termination. Somewhat finer patterns are observed in Fig. 6,

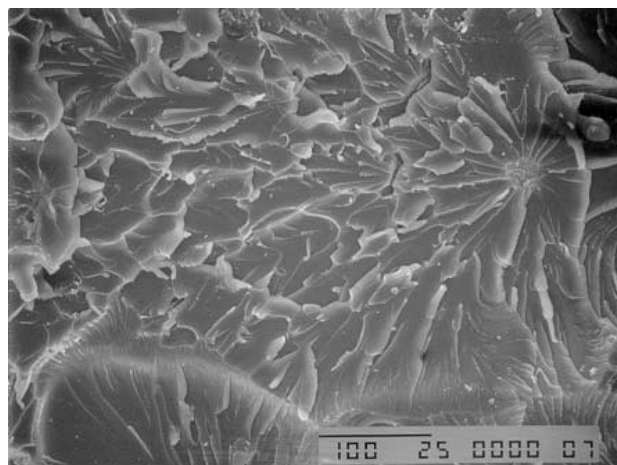


Fig. 6. Fracture surface of DGE-DHBP (scale: 100 μm).

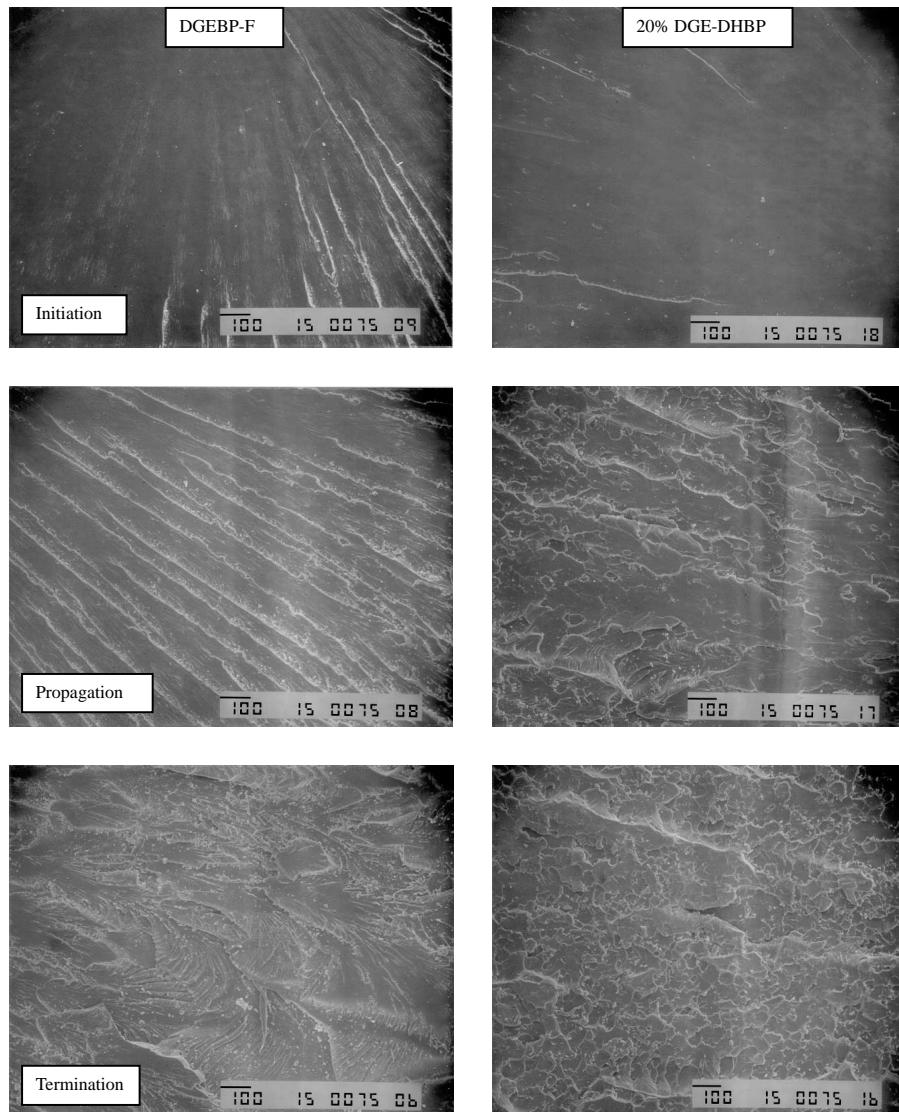


Fig. 7. Comparison of fracture structure of pure DGEBP-F and the system containing 20% DGE-DHBP ($75\times$) (scale: 100 μm).

reminiscent of those by Sue and coworkers [59] for their LC epoxies.

The comparison of fractography of pure DGEBP-F and the system containing 20% DGE-DHBP is shown in Fig. 7. We observe a river pattern where the multiple lines begin as a single line at the initiation point. The fracture surfaces of the tensile specimens for modified and unmodified systems exhibit marked differences in the areas of rapid crack growth. Our micrographs do not show discontinuous fracture propagation observed by d'Almeida and Monteiro for their epoxies based on diglycidyl ether of bisphenol A and triethylene tetramine hardener [60]. However, they did not have a LC component and they added on a higher concentration of the hardener to cure the epoxy. The main region, which reflects differences in deformation, is the termination region. The stability of the crack growth regions varies with DGE-DHBP concentration. Higher surface roughness is connected with higher energy required to

fracture the specimens. The fracture surface of DGE-DHBP also shows high roughness. However, the toughness observed is lower than expected. This is due to the large area of the rapid crack propagation region as compared to the initiation region.

6. Mechanism of crack propagation

The mechanical properties and morphology results reported in Section 5 imply that there are differences in fracture mechanisms in unmodified and modified systems. Fig. 8 presents the optical micrograph of the crack tip of an unmodified sample. The crack path in DGEBP-F cured with MTPA is a straight line. This is an indication of brittle fracture. Some areas of crack bridging are observed. However, they are not dominant in affecting the fracture toughness.

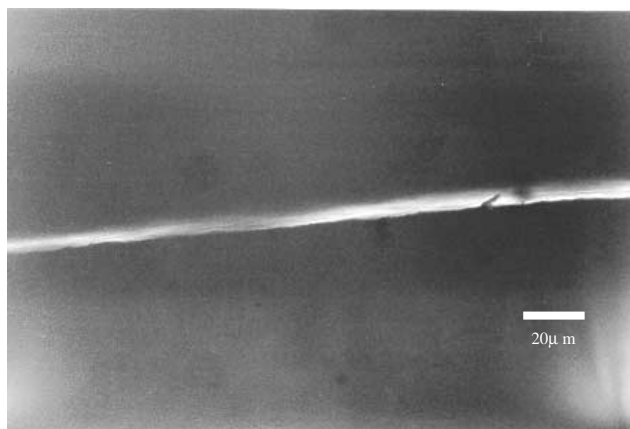


Fig. 8. Optical micrograph of a crack area of cured DGEBP-F with MTHPA.

The crack propagating mechanism for 10% DGE-DHBP in DGEBP-F cured with MTHPA is presented in Fig. 9. As reported in Section 4, the mechanical properties at this concentration provide the highest improvement in strength. The main mechanism found in this case is crack deflection. This might be the effect of the mesogenic units distributed in the network. The fracture route follows along the LC edge so the deflection of crack in the sub-fracture surface zone is found.

7. Concluding remarks

The presence of DGE-DHBP enhances the toughness of the blended epoxy samples without decreasing the modulus of sample — as observed by tensile and impact tests as well as reflected in the morphology observed from SEM pictures of fracture surfaces. Moreover, the results show that for all compositions the glass transition temperature is increased relative to the pure epoxy component, hence they have potential for high temperature applications. Curing both components in situ with the same curing agents is a proces-

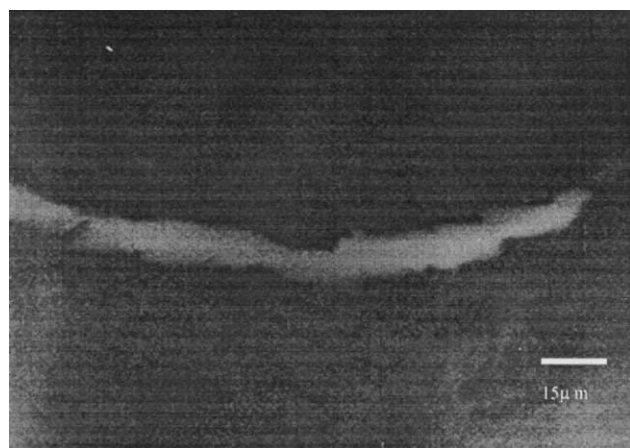


Fig. 9. Optical micrograph of a crack area of cured 10% DGE-DHBP in DGEBP-F + MTHPA.

ing advantage. Compared to alternative toughening methods such as rubber toughening and thermoplastic addition, the magnitude of the increase in fracture toughness is not high. However retention of modulus is a definite advantage here and processing is not subject to lamination arising from viscosity gradients. We postulate that changing the glass transition and chain mobility of the base epoxy is a significant factor in affecting large-scale changes in fracture toughness.

Relatively small amounts of the LC epoxy (DGE-DHBP) can be used as an additive to improve toughness of a non-LC epoxy for high performance applications. Benefits are obtained without necessarily an LC phase formation. The maximum of the area under the stress–strain curve at 10% DGE-DHBP can be explained in terms of the disruption of the epoxy network packing creating additional free volume. However, a further increase of the DGE-DHBP concentration results in local formation of the structure based on the added component. Thus, it is primarily the perturbation of the structure of the pure component, which enhances toughness at low LC concentrations.

The main mechanism of the 10% DGE-DHBP in DGEBP-F cured with MTHPA is crack deflection and curve fracture. The curve fracture increases the surface area of the crack and improves the toughness. This is the effect of the mesogenic units distributed in the network.

Acknowledgements

Financial support has been provided by the State of Texas Advanced Technology and Advanced Research Program (Project # 003594-077 and 003594-075). Equipment donation by the Perkin–Elmer Corp. is acknowledged also. We gratefully acknowledge David Garrett for help with SEM experiments and H.J. Sue for double-notch four point bending test.

References

- [1] Arends CB. Polymer toughening. New York: Marcel Dekker, 1996.
- [2] Kirshenbaum SL. In: Riew CK, editor. Rubber-modified thermoset resins. Washington, DC: American Chemical Society, 1984. p. 163.
- [3] Riew CK. Rubber-toughened plastics. Advances in Chemistry Series 222. Washington, DC: ACS, 1989.
- [4] Riew CK, Kinloch AJ. Toughening Plastics I. Advances in Chemistry Series 233. Washington, DC: ACS, 1993.
- [5] Riew CK, Kinloch AJ. Toughening Plastics II. Advances in Chemistry Series 252. Washington, DC: ACS, 1996.
- [6] Klempner D, Sperling LH, Utracki LA. Interpenetrating polymer networks. Advanced in Chemistry Series 239. Washington, DC: ACS, 1994.
- [7] Sperling LH. Interpenetrating polymer networks and related materials. New York: Plenum Press, 1981.
- [8] Prakash NA, Liu YM, Jang BZ, Wang JB. Polym Compos 1994;15:479.
- [9] Kinloch AJ, Young RJ. Fracture behavior of polymers. New York: Elsevier, 1985.

- [10] Sultan JN, McGarry FJ. *Polym Engng Sci* 1973;13:29.
- [11] Parker DS, Sue HJ, Huang J, Yee AF. *Polymer* 1990;31:2267.
- [12] Sue HJ. *Polym Engng Sci* 1991;31:275.
- [13] Girard-Reydet E, Sautereau H, Pascaut JP, Keates P, Navard P, Thollet G, Vigier G. *Polymer* 1998;39:2269.
- [14] Bauer RS, editor. *Epoxy resin chemistry II. Advances in Chemistry Series*, vol. 221. Washington, DC: ACS, 1984.
- [15] Ho TH, Wang CS. *J Appl Polym Sci* 1993;50:477.
- [16] Buner IR, Rushford IL, Rose WS, Hunston DL, Riew CK. *J Adhes* 1982;13:242.
- [17] Pearson RA, Yee AF. *J Appl Polym Sci* 1992;48:1051.
- [18] Kunz SC, Sayre JA, Assink RA. *Polymer* 1987;23:1897.
- [19] Han X, Yun Z, Guo F. *Mater Res Soc Symp Proc* 1992;274:11.
- [20] Bucknall CB, Partridge IK. *Polymer* 1983;24:639.
- [21] Diamont I, Moulton RJ. *SAMPE Int Symp* 1984;29:422.
- [22] Raghava RS. *J Polym Sci Phys* 1987;25:1017.
- [23] Recker HG, Allspach T, Altstadt V, Folda T, Heckmann W, Ittemann P, Tesch H, Weber T. *SAMPE Quart* 1989;21:46.
- [24] Hedrick JL, Yilgor I, Jurek M, Hedrick JC, Wilkes GL, McGrath JE. *Polymer* 1991;32:2020.
- [25] Min BG, Stachurski ZH, Hodgkin JH. *J Appl Polym Sci* 1993;50:1511.
- [26] Barclay GG, Ober CK. *Prog Polym Sci* 1993;18:899.
- [27] Muller HP, Gipp R, Heine H. US Patent 4, 764, 581, 1988.
- [28] Earls JD, Hefner RE, Puckett PM. US Patent 5, 218, 062, 1993.
- [29] Giamberini M, Amendola E, Carfagna C. *Mol Cryst Liq Cryst* 1995;266:9.
- [30] Weiss R, Ober CK, editors. *Liquid crystalline polymers: chemistry, structure and properties*. Washington DC: American Chemical Society, 1990.
- [31] Carfagna C, Amendola E, Giamberini M, Hakemi H, Pane S. *Polym Int* 1997;44:465.
- [32] Carfagna C, Amendola E, Giamberini M. *Prog Polym Sci* 1997;22:1607.
- [33] Sue HJ, Earls JD, Hefner RE. *J Mater Sci* 1997;32:4031.
- [34] Punchaipetch P, Ambrogi V, Giamberini M, Brostow W, Carfagna C, D'Souza NA. *Polymer* 2001;42:2067.
- [35] Hefner RE, Jr., Earls JD, Puckett PM. US patent 5, 266, 660, 1993
- [36] Tada H, Paris PC, Irwin GR. *The stress analysis of cracks handbook*. 2nd ed. St. Louis: Paris Productions, 1985.
- [37] Anderson TL. *Fracture mechanics fundamental and applications*. Boca Raton: CRC Press, 1995.
- [38] Sue HJ, Pearson RA, Parker DS, Huang J, Yee AF. *Polymer Preprints*. ACS 1988;29:147.
- [39] Sue HJ, Yee AF. *J Mater Sci* 1993;28:2951.
- [40] Ting RY. In: May CA, editor. *Epoxy resins: chemistry and technology*. New York: Marcel Dekker, 1988.
- [41] Coleman MM, Serman CJ, Bhagwagar DF, Painter PC. *Polymer* 1990;31:1187.
- [42] Daubert TE, Danner RP. *Data compilation: tables of properties of pure compounds*. New York: American Institute of Chemical Engineering, 1989.
- [43] Kline DE. *J Polym Sci* 1960;47:237.
- [44] Homes AH. PhD Dissertation, Texas A and M 1992.
- [45] McCrum N, Williams B, Read G. *Anelastic and dielectric effects in polymeric solids*. New York: Dover, 1991.
- [46] Menard KP. *Dynamic mechanical analysis: a practical introduction*. Boca Raton: CRC Press, 1999.
- [47] Lin Q, Yee AF. *Polymer* 1994;35(2):2679.
- [48] Ortiz C, Kim R, Rodighiero E, Ober CK, Kramer EJ. *Macromolecules* 1998;31:4074.
- [49] Punchaipetch P. PhD Dissertation, University of North Texas 2000.
- [50] Dealy JM, Wissbrun KF. *Melt rheology and its role in plastics processing*. Great Britain: Chapman and Hall, 1995.
- [51] Nielson IE. *Mechanical properties of polymer and composites*. New York: Marcel Dekker, 1975.
- [52] Tobolsky AV. *Properties and structure of polymers*. New York: Wiley, 1960.
- [53] Blonski S, Brostow W, Jonah DA, Hess M. *Macromolecules* 1993;26:84.
- [54] Brostow W, Hess M, Lopez B, Sterzynski T. *Polymer* 1996;37:1551.
- [55] Brostow W, Hess M, Lopez BL. *Macromolecules* 1994;27:2262.
- [56] Brostow B, Dziemianowicz TS, Romanski J, Werber W. *Polym Engng Sci* 1988;28:785.
- [57] Martinez I, Martin MD, Eceiza A, Oyanguren P, Mondragon I. *Polymer* 2000;41:1027.
- [58] Bagheri R, Williams MA, Pearson RA. *Polym Engng Sci* 1997;37:245.
- [59] Sue HJ, Earls JD, Hefner RE. *J Mater Sci* 1997;32:4039.
- [60] D'Almeida JRM, Monteiro SN. *J Polym Engng* 1998;18:235.